Molecular Genetics and Metabolism 115 (2015) 110–117

Contents lists available at ScienceDirect

Molecular Genetics and Metabolism

journal homepage: www.elsevier.com/locate/ymgme

Novel missense mutations in *PNPLA2* causing late onset and clinical heterogeneity of neutral lipid storage disease with myopathy in three siblings

Sara Missaglia [a,1], Elisabetta Tasca [b,1], Corrado Angelini [b], Laura Moro [c], Daniela Tavian [a,d,*]

[a] Laboratory of Cellular Biochemistry and Molecular Biology, CRIBENS, Catholic University of the Sacred Heart, Milan, Italy
[b] Fondazione Ospedale San Camillo IRCCS, Lido, Venice, Italy
[c] Department of Pharmaceutical Sciences, University of Piemonte Orientale "A. Avogadro", Novara, Italy
[d] Psychology Department, Catholic University of the Sacred Heart, Milan, Italy

ARTICLE INFO

Article history:
Received 30 April 2015
Accepted 1 May 2015
Available online 2 May 2015

Keywords:
Neutral lipid storage disease
Myopathy
Hepatosteatosis
Diabetes mellitus
Lipase
Trialcylglycerol
Lipid droplets

ABSTRACT

Neutral lipid storage disease with myopathy (NLSD-M) is a rare autosomal recessive disorder characterised by an abnormal accumulation of triacylglycerol into cytoplasmic lipid droplets (LDs). NLSD-M patients are mainly affected by progressive myopathy, cardiomyopathy and hepatomegaly. Mutations in the *PNPLA2* gene cause variable phenotypes of NLSD-M. *PNPLA2* codes for adipose triglyceride lipase (ATGL), an enzyme that hydrolyses fatty acids from triacylglycerol. This report outlines the clinical and genetic findings in a NLSD-M Italian family with three affected members. In our patients, we identified two novel *PNPLA2* missense mutations (p.L56R and p.I193F). Functional data analysis demonstrated that these mutations caused the production of ATGL proteins able to bind to LDs, but with decreased lipase activity. The oldest brother, at the age of 38, had weakness and atrophy of the right upper arm and kyphosis. Now he is 61 years old and is unable to raise arms in the horizontal position. The second brother, from the age of 44, had exercise intolerance, cramps and pain in lower limbs. He is currently 50 years old and has an asymmetric distal amyotrophy. One of the two sisters, 58 years old, presents the same *PNPLA2* mutations, but she is still oligo-symptomatic on neuromuscular examination with slight triceps muscle involvement. She suffered from diabetes and liver steatosis. This NLSD-M family shows a wide range of intra-familial phenotypic variability in subjects carrying the same mutations, both in terms of target-organs and in terms of rate of disease progression.

1. Introduction

NLSD-M (MIM 610717) and NLSD-I (neutral lipid storage disease with ichthyosis, MIM 275630) are due to mutations in adipose triglyceride lipase (ATGL) or in α/β-hydrolase domain-containing protein 5 (ABHD5) and are characterised by systemic triacylglycerol deposition in cytoplasmic lipid droplets (LDs) in most tissues, including skeletal and cardiac muscles, liver and peripheral blood [1]. LDs are virtually present in all cell types, representing a reservoir of bioactive lipids and lipid-derived hormones in adipose and non-adipose tissues [2]. The white blood cell diagnostic feature of NLSD is characterised by lipid-containing vacuoles in leukocytes, which was originally described by Jordans [3,4]. Clinically, the main difference between NLSD-I and NLSD-M is that a lack of ABHD5 results in early ichthyosis and often liver involvement whereas a lack of ATGL essentially causes the predominant clinical phenotype with skeletal and cardiac myopathy [1].

In particular, NLSD-M patients are characterised by progressive myopathy (100%), cardiomyopathy (44%), elevated serum creatine kinase (100%), hepatomegaly (20%), diabetes (24%), chronic pancreatitis (14%) and short stature (15%) [5–11]. No ichthyosis is observed in patients suffering from NLSD-M, even though the skin of few patients appears to be particularly dry [12].

The onset of NLSD-M is caused by mutations in the *PNPLA2* gene, which codes for ATGL, a member of the patatin-like phospholipase domain-containing proteins [5]. This lipase is a lipid droplet-associated protein and catalyses the first step in the hydrolysis of triacylglycerols (TGs), stored within LDs [1] thereby generating diacylglycerols and free fatty acids.

The human ATGL protein consists of 504 amino acids divided into a N-terminal part containing the patatin domain (amino acids 10 to 178) with catalytic residues S47 and D166 and a C-terminal part containing a hydrophobic lipid binding domain at position 315–360. ATGL's enzymatic activity is co-activated by ABHD5, a 39 kDa protein that associates with LDs, and inhibited by the protein G0G1 switch gene 2 (G0S2). The

* Corresponding author at: Laboratory of Cellular Biochemistry and Molecular Biology, CRIBENS, Catholic University of the Sacred Heart, pz Buonarroti 30, 20145 Milan, Italy.
E-mail address: daniela.tavian@unicatt.it (D. Tavian).
[1] Both of these authors contributed equally to this work and should be considered as first authors.

http://dx.doi.org/10.1016/j.ymgme.2015.05.001

254-N-terminal residues of ATGL are required for TG hydrolysis and for regulatory interactions with its co-activator ABHD5 and its inhibitor G0S2 [13].

To the best of our knowledge, 41 NLSD-M patients have been clinically and genetically characterised [5,14–21]. Twenty-seven different *PNPLA2* mutations, which could differently affect protein function or production, have been described. Here, we report the clinical and genetic findings of a NLSD-M family of Italian origin with three affected siblings. Moreover, in order to highlight the effect that different gene mutations may have on ATGL lipase activity, we have performed a functional characterisation of the novel *PNPLA2* missense mutations identified in our patients.

2. Materials and methods

2.1. Muscle histopathology

Histopathological evaluation of muscle was performed according to the standard procedures described by Dubowitz [22]. Light microscopy of frozen cross sections of muscle biopsies was used for conventional histochemical and histoenzymatic stains, including haematoxylin & eosin (H&E), Gomori trichrome, Oil-Red-O (ORO), NADH-TR, COX, SDH, acid phosphatase, acid and alkaline ATPases.

2.2. Cell culture

Fresh EDTA-treated peripheral blood samples (3 mL) from patients were centrifuged at 3300 *g* for 10 min. Buffy coats were carefully collected by gentle pipette suction, immediately smeared onto slide glasses, completely dried, and fixed with Biofix (Bio-Optica, Milan, Italy). May-Grünwald–Giemsa (MGG) staining was carried out according to the standard procedures. Human skin fibroblasts from patients were obtained from skin biopsies and cultured in Earle's minimum essential media (MEM) with 10% foetal bovine serum (FBS), 100 IU/mL penicillin and 100 mg/mL streptomycin at 37 °C in a 5% CO_2 incubator. Fibroblasts were observed under phase-contrast light microscopy and photographed (40×; I X51, Olympus).

Fibroblasts (200,000 per dish) were also seeded on coverslips in Earle's MEM culture medium and allowed to adhere for 36 h. The medium was then removed and cells were washed with Dulbecco's phosphate-buffered saline (D-PBS), stained with Nile Red dye (NR, 9-diethylamino-5Hbenzo[alpha]phenoxazine-5-one) and examined with a Leica MB5000B microscope equipped with 20×, 40× and 100× oil immersion objectives. Fluorescence images were captured using a Leica DFC480 R2 digital camera and a Leica Application Suite (LAS) software.

2.3. Molecular analysis

Genomic DNA was extracted from peripheral blood using a Puregene DNA Isolation kit (Qiagen, Venlo, Netherlands). Primer sequences and PCR amplification conditions for the analysis of *PNPLA2* coding regions (GenBank NM02376) were previously reported [5]. All PCR products were purified (NucleoSpin Extract II, Macherey-Nagel, Germany) and sequenced on 3730 DNA analyser by the BigDyew Terminator V1.1 Cycle sequencing kit (Applied Biosystems, Foster City, CA, USA).

Informed consent for genetic and histological analysis was obtained from participants of the study. Moreover, written informed consent from the patients was obtained for publication of the article and any accompanying images.

2.4. Generation of site-directed mutagenesis PNPLA2 plasmids and expression of recombinant mutants in HeLa cells

PNPLA2 cDNA has been previously cloned into pEGFP-N1 from Clontech (Mountain View, CA, USA) to produce pEGFPN1-*PNPLA2*, expressing ATGL with GFP at the C-terminus. Point mutations were performed using the Phusion Site-Directed Mutagenesis Kit (Thermo Scientific, Waltham, MA, USA). Mutations in pEGFP-*PNPLA2* plasmid were introduced using the following primers: S47A: forward 5′-CACA TCTACGGCGCCGCGGCCGGGGCGCTCACGG-3′ and reverse: 5′-CCGTGA GCGCCCCGGCCGCGGCGCCGTAGATGTG-3′; L56R: forward 5′-GCCACG GCGCGGGTCACCGGGG-3′ and reverse 5′-CCCCGGTGACCCGCGCCGTG GC; I193F: forward 5′-CGGGCGAGAGTGACTTCTGTCCGCAGGAC and reverse 5′-GTCCTGCGGACAGAAGTCACTCTCGCCCG. All constructs were verified by DNA sequencing.

HeLa cells were cultured on glass coverslips in Dulbecco's modified Eagle's medium with 10% FBS. 400 μM oleate complexed to BSA (6:1 molar ratio) was added to the medium and incubated overnight. The cells were then transiently transfected with control and recombinant *PNPLA2* plasmids using the Lipofectamine 2000 transfection reagent, according to the manufacturer's protocol (Life Technologies, Carlsbad, CA, USA). After 24 h, the cells were fixed and stained with ORO, and LDs from immunofluorescent images were examined with a Leica MB5000B microscope. Fluorescence images were captured using a Leica DFC480 R2 digital camera and a LAS software. Moreover, fluorescence images were also captured using a confocal microscope Leica TCS SPE equipped with 63× oil immersion objective.

2.5. Triglyceride quantification in NLSD-M fibroblasts and HeLa transfected cells

NLSD-M and control fibroblasts at the same passage (P8) were seeded onto plates at a density of 1×10^6 cells/plate and cultured as previously described. The day after, the cells were homogenised in 1 mL solution containing 5% TRITON X-100 (Sigma-Aldrich, Saint Louis, MO, USA), incubated at 80 °C for 5 min and centrifuged for 2 min. Cellular triglyceride content was quantified using Triglyceride Quantification Colorimetric Kit (Biovision, Milpitas, CA, USA), according to the instructions. The absorbance was measured at 570 nm with EnVision Multilabel Reader (PerkinElmer, Waltham, MA, USA).

5×10^5 HeLa transfected cells were cultured in DMEM with 10% FBS and supplemented with 400 μM oleate/BSA, and allowed to adhere overnight. The day after, the cells were transiently transfected, as explained in paragraph 2.4. After 24 h, the cells were homogenised and cellular triglyceride content was quantified using Triglyceride Quantification Colorimetric Kit. Intracellular TG content was expressed as nanomoles of TG per milligrammes of cellular protein.

2.6. Statistical and bio-informatic analysis

The statistical analysis of quantitative data on LDs identified from cells (fibroblasts and HeLa transfected cells) by image analysis of immunofluorescence experiments was made using SPSS v.19 package (SPSS, Chicago, IL, USA). The values were compared using x^2-squared test. A P-value of ≤ 0.05 was considered to be statistically significant.

The effect of amino acid substitutions on protein function was predicted using ClustalW, SIFT and PolyPhen software. A multiple sequence alignment of mammalian ATGL proteins was used as input for ClustalW. The NCBI reference sequence (NP_065109.1) of the human ATGL protein was used as the input for SIFT and PolyPhen, with default query options.

3. Results

3.1. Patient description

Family's pedigree is showed in Fig. 1A.

3.1.1. Patient 1

The oldest brother is now 61 years old (Fig. 1B). He worked as a clerk for the rail network, although from the age of 40 he complained of becoming easily fatigued. From the age of 38, he had weakness and

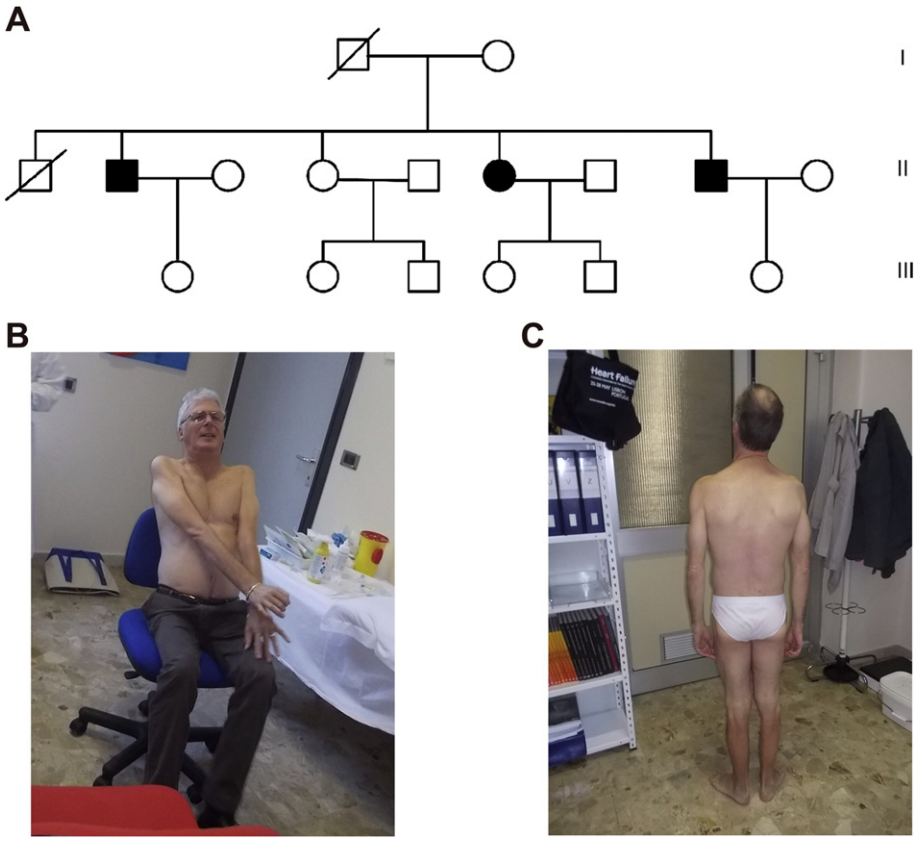

Fig. 1. Clinical phenotype of NLSD-M patients. (A) Pedigree of the NLSD-M family; (B) patient II-1; (C) patient II-3.

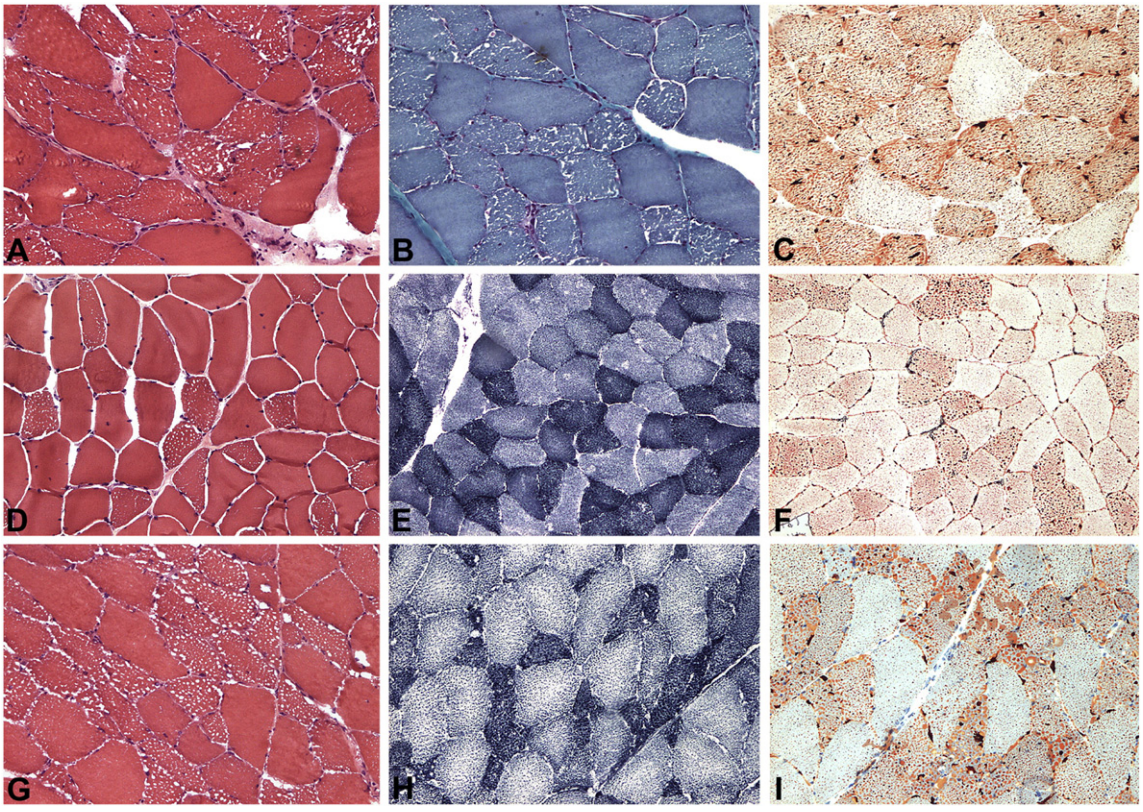

Fig. 2. Muscle histopathology of two biopsies from patient II-1 (first biopsy, A,B,C; second biopsy D, E, F) and one biopsy from patient II-3 (G, H, I), stained with haematoxylin–eosin (A, D, G), Gomori trichrome (B), NADH-TR reductase (E, H) and Oil-Red-O (C, F, I).

hypotrophy in the right upper arm and kyphosis. One year later, he underwent surgery for an abdominal teratoma. At the age of 50 years, he experienced painful cramps in the arms especially after exercise. Moreover, he complained of pain and rigidity to his right leg. He presented upper limb weakness at the age of 60 and he is now unable to raise arms in the horizontal position (15 °C) and presents severe weakness in his upper limbs with diffuse atrophy, more marked in right deltoid, biceps and triceps muscles (Fig. 1B). Spirometry showed a restrictive ventilatory insufficiency (forced vital capacity = 57%). Plasma creatine kinase (CK) values varied between 804 and 1118 IU/L (normal values: 0–180 IU/L). Muscle biopsy from the deltoid was performed at the age of 39; it showed lipid droplet accumulation positive with Oil-Red-O staining (Fig. 2C, patient II-1), suggesting a lipid storage myopathy. Moreover, vacuolated fibres were detected using H&E and Gomori trichrome staining (Fig. 2A and B). At the age of 40, he underwent a biopsy of the quadriceps; Oil-Red-O staining revealed a lipid abnormal storage, Gomori trichrome staining evidenced a lower degree of fibre vacuolisation, and NADH-TR stain showed some atrophic fibres and irregular staining (Fig. 2E and F). The patient had normal plasma and urine carnitine levels, but a low total plasma carnitine (27.9 nanomoles/mL; normal 36.2–72.9 nanomoles/mL). Liver function tests revealed mildly elevated values of aspartate aminotransferase (AST = 79U/L, normal range 4–40) and alanine aminotransferase (ALT = 72 U/L, normal range 4–40), while normal values of gamma glutamyl transpeptidase (GGT), serum albumin and bilirubin were found. A mild hypercholesterolemia was noted (222 mg/dL, normal range <200). EMG was myopathic.

At the age of 59, an abdominal ultrasound showed a mild hepatic steatosis with liver enlargement. ECG and cardiac ultrasound were normal.

3.1.2. Patient 2

This is the 50 year-old brother of patient II-1.

From the age of 35, he had exercise intolerance, cramps and pain in lower limbs, especially in the right calf, and had scoliosis and scapular winging (Fig. 1C). A muscle biopsy was taken from the quadriceps at the age of 37. Vacuoles were detected using H&E and Oil-Red-O stain and atrophic type I fibres reactive using NADH-TR stain (Fig. 2G, H and I). In the same period he developed a progressive weakness of the right arm. He currently has an asymmetric distal amyotrophy. His plasma CK level was 1389 U/L, while serum hypertriglycerides (176 mg/dL, normal range <175) and cholesterolemia (208 mg/dL, normal range <200) were in upper limits. Liver function tests revealed slightly elevated values of aspartate aminotransferase (AST = 45 U/L, normal range 4–40) and alanine aminotransferase (ALT = 57 U/L, normal range 4–40).

3.1.3. Patient 3

Patient 3 is the sister of the two above brothers. She is presently 58 years old.

For many years, she suffered from diabetes mellitus and required insulin therapy. The last examination revealed blood glucose levels of 305 mg/dL (normal range 70–110) and plasma parameters for ALT, AST, and GGT were elevated indicating impaired liver function. Cholesterol and triglycerides were also elevated (298 mg/dL and 274 mg/dL, respectively). An abdominal ultrasound showed a hyperechogenic liver, for which she underwent a liver biopsy that revealed hepatic steatosis. Her CK value was 724 U/L. Currently, she has mild weakness in her right triceps brachii muscle, but in other muscles she has normal strength.

All three siblings showed Jordans' anomaly (Fig. 3A) in leukocytes and abnormal lipid storage into LDs in skin fibroblasts (Fig. 3B and C).

The intracellular TG content from patients and control fibroblasts has been determined in order to show the degree of LD accumulation. As expected, the TG content in fibroblasts from patients was significantly higher than in control fibroblasts ($P < 0.001$) (Supplementary Fig. 1). There was also a significant difference in the TG amount between the oldest patient II-1 and the other two (patient II-2 and patient II-3; $P < 0.001$; $P < 0.05$), while no significant difference was detected between patient II-2 and patient II-3 ($P = 0.417$).

3.2. Genetic analysis

Sequencing of the *PNPLA2* gene confirmed the suspected clinical diagnosis of NLSD-M. Our patients were compound heterozygotes for two novel missense mutations, c.177T>G (p.L56R) and c.577A>T (p.I193F) (Fig. 4A and B). These mutations were not observed in 200 alleles from control subjects, and they were submitted to GenBank (accession numbers: KF833264 and KF833265). The first mutation (p.L56R) is localised in the catalytic site, very near to serine 47, which is part of the catalytic dyad of ATGL (Fig. 4C and D). The second variation (p.I193F) is localised in a region close to the patatin domain (Fig. 4C and D). A multiple sequence alignment of mammalian ATGL proteins revealed complete conservation of leucine 56 and isoleucine 193 (Fig. 2S). Moreover, according to bio-informatic prediction tools (SIFT and PolyPhen-2), the p.L56R and the p.I193F mutations are to be considered as "damaging" (Fig. 2S).

3.3. Functional study of missense PNPLA2 mutations

To verify the pathogenic effect of the *PNPLA2* allelic mutations identified in our patients, we constructed different recombinant plasmids expressing ATGL fused to a GFP tag. The plasmids contained either human *PNPLA2* cDNA (p*PNPLA2*-EGFP), human *PNPLA2* with the p.L56R mutation (p*PNPLA2*-L56R-EGFP) and human *PNPLA2* with the p.I193F mutation (p*PNPLA2*-I193F-EGFP). For comparison, we have previously constructed human *PNPLA2* with p.S47A mutation. S47 amino-acid is located in the core of catalytic domain and is essential for enzyme activity. We observed in HeLa cells transfected with both wild type p*PNPLA2*-GFP or mutated *PNPLA2* plasmids, that all ATGL proteins were able to bind to LDs (Fig. 5A). Furthermore the correct localization of ATGL mutant proteins on LD surface has been clearly highlighted by confocal microscopy images (Fig. 5B). While transfection with the positive control (p*PNPLA2*-EGFP) strongly reduced the number and area of the LDs, transfection of the mutant plasmids p*PNPLA2*-L56R-EGFP and p*PNPLA2*-I193F-EGFP has a significant minor effect ($P < 0.001$) (Fig. 5, graphs C and E). The *PNPLA2* mutations identified in our patients (p.L56R and p.I193F) maintain a residual enzymatic activity (L56R: number of LDs per cells 29%, area of LD sections 27%; I193F: number of LDs per cells 39%, area of LD sections 38%) if compared to p*PNPLA2*-S47A-EGFP, considered as totally inactive. The level of activity of ATGL(S47A) is significantly lower in comparison with those of the L56R and I193F mutant proteins ($P < 0.001$) (Fig. 5, graphs D and F).

In agreement with data obtained from quantitative analysis of immunofluorescence images (Fig. 5C and E), the intracellular TG content in HeLa cells overexpressing GFP tagged mutants and wt ATGL confirms that ATGL(L56R) and ATGL(I193F) proteins present a residual lipase activity (Fig. 5G). Furthermore, a slight difference between the two mutations identified in our family is evidenced. The ATGL(L56R) seems to be mostly impaired with respect to ATGL(I193F) (Fig. 5C, E and G). The statistical analysis that compares data from graphs C, E and G has been reported (Fig. 5D, F and H). The number of LDs per cell in ATGL(I193F) mutant is significantly lower than ATGL(L56R) ($P < 0.05$) (Fig. 5D). Concerning the data relative to the area of LD sections and the TG content, the difference between ATGL(I193F) and ATGL(L56R) has the same trend, although not statistically significant ($P = 0.292$ and $P = 0.262$ respectively) (Fig. 5F and H).

4. Discussion

Until now, eight different *PNPLA2* missense mutations have been identified in NLSD-M patients. They represent almost 25% of gene variations and are mainly localised in the patatin domain of the protein, or very close to it. With the exception of those described in this study,

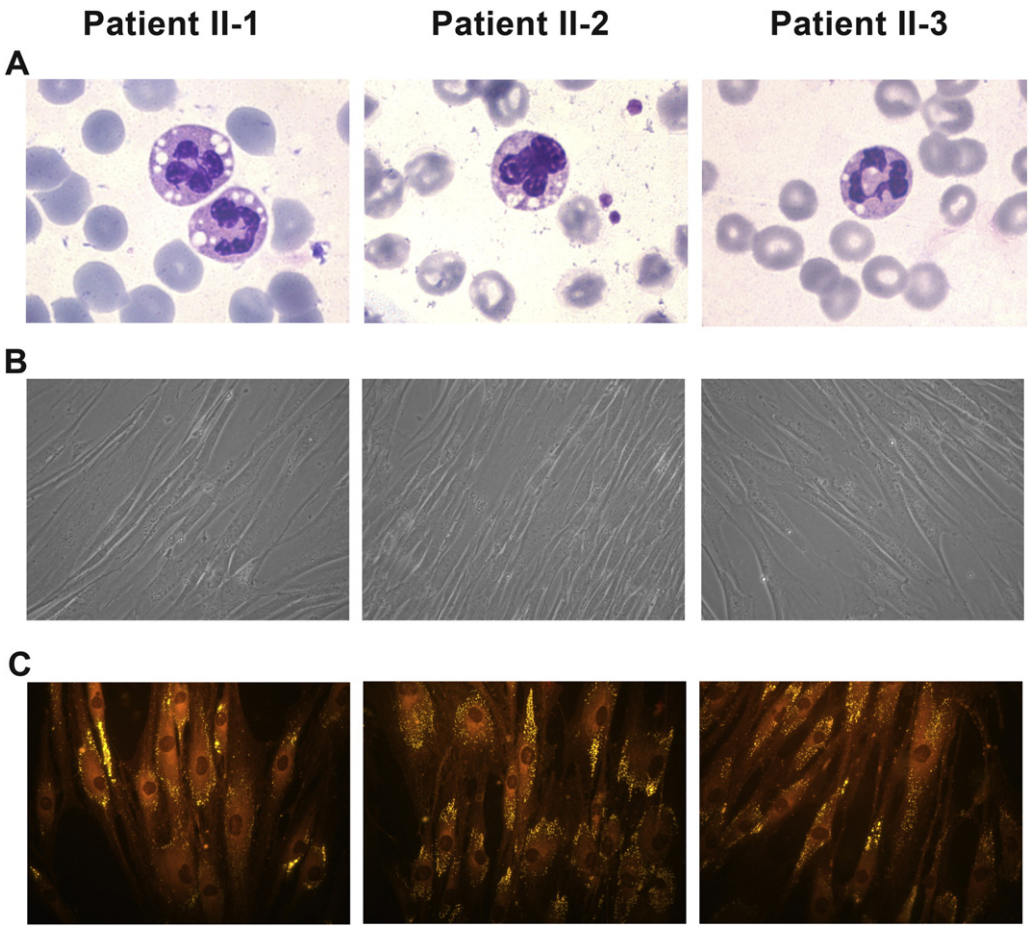

Fig. 3. Histochemical characterization of NLSD-M patients. (A) Microphotographs of Jordans' bodies in patient's buffy coats stained with May-Grünwald Giemsa (100× magnification); (B) cultured fibroblasts from affected patients (II-1, II-2 and II-3), phase contrast images (40× magnification); (C) cultured fibroblasts from affected patients (II-1, II-2 and II-3), fluorescent microscopy images with Nile red staining (40× magnification).

they have been detected in a homozygous status or associated with truncating mutation. Here, we have reported a NLSD-M Italian family with three affected siblings, which are compound heterozygotes for two novel *PNPLA2* missense mutations. The p.L56R is located near the residue S47 of ATGL catalytic dyad, while the second one, p.I193F, in a highly conserved amino acid sequence near the patatin region. Our

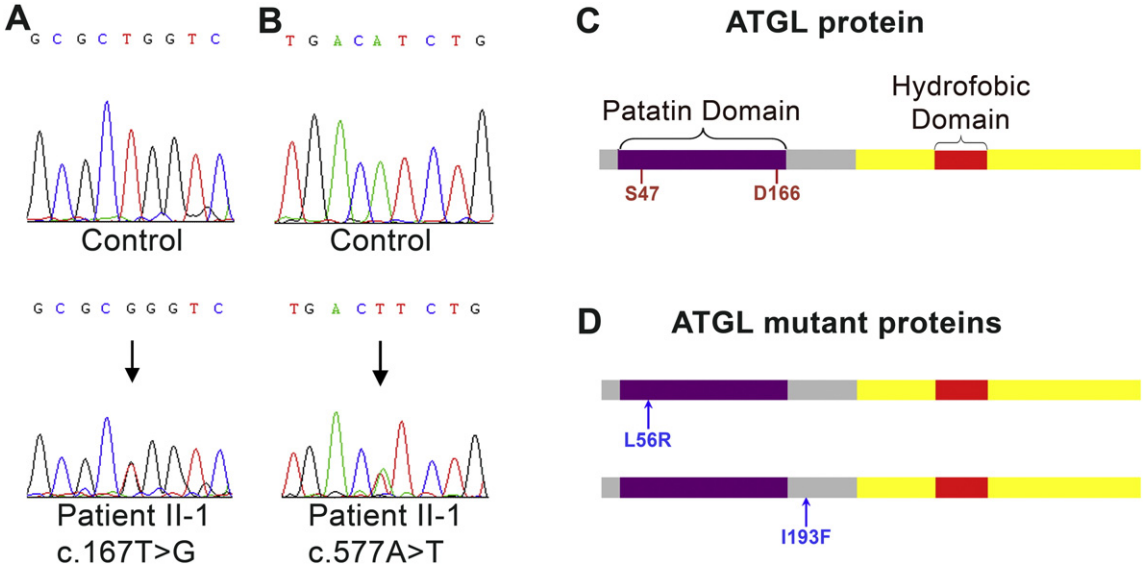

Fig. 4. Identification of *PNPLA2* mutations. (A,B) Electropherograms of *PNPLA2* exon 2 and exon 5 showing the c.167T>G and the c.577A>T mutations. (C) Structural domains of ATGL protein. The patatin domain is located between amino acids I10 and L178 and contains the catalytic dyad (S47 and D166). The hydrophobic domain (P315–P360) is the LD-binding region. (D) Schematic representation of ATGL mutant proteins. In the scheme, the localisation of the amino acid substitutions is reported: the p.L56R mutation falls into the patatin domain (I10–L178), while the p.I193F mutation is localised close to the same region.

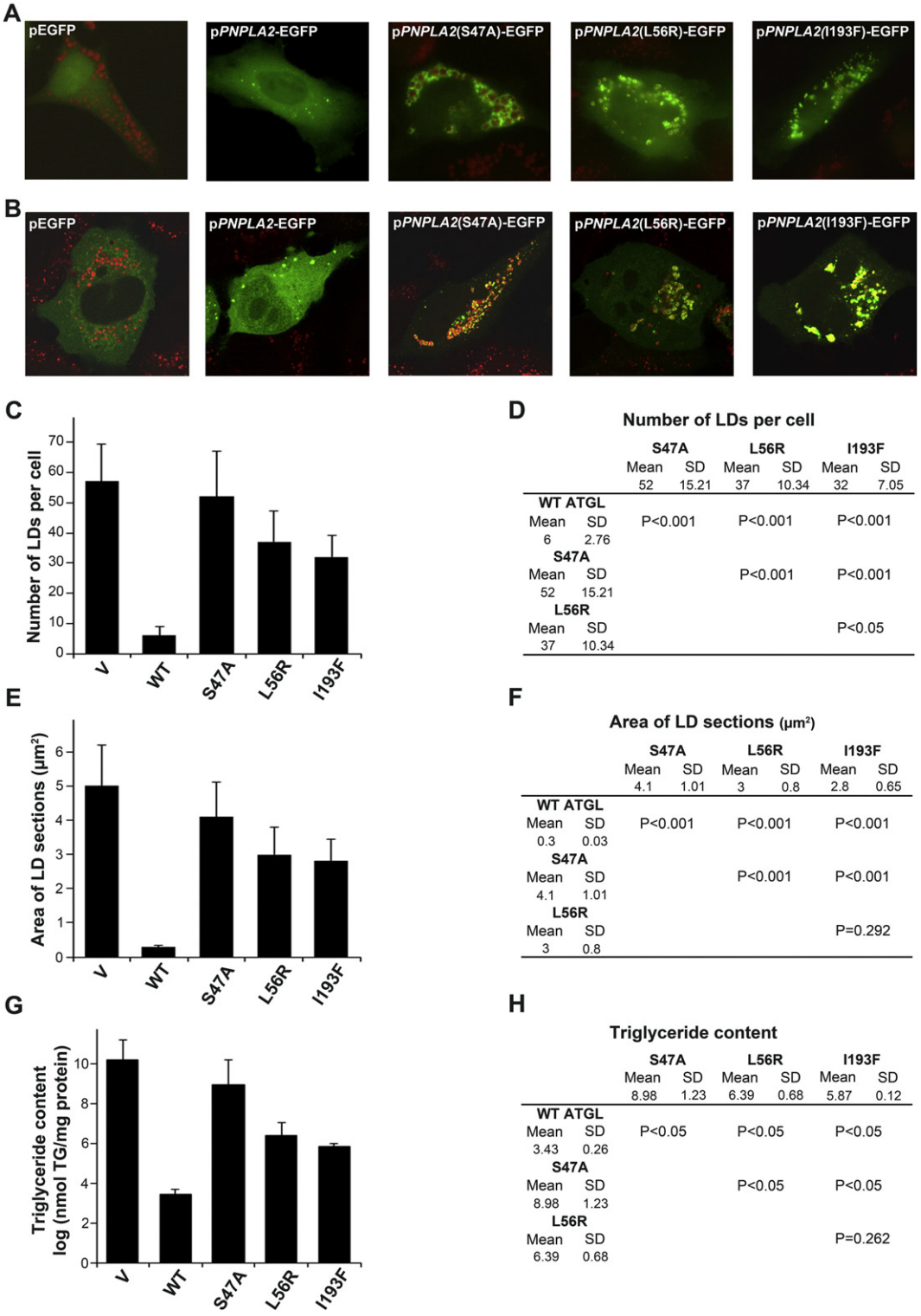

D

	S47A Mean	S47A SD	L56R Mean	L56R SD	I193F Mean	I193F SD
	52	15.21	37	10.34	32	7.05
WT ATGL						
Mean SD	P<0.001		P<0.001		P<0.001	
6 2.76						
S47A						
Mean SD			P<0.001		P<0.001	
52 15.21						
L56R						
Mean SD					P<0.05	
37 10.34						

F

	S47A Mean	S47A SD	L56R Mean	L56R SD	I193F Mean	I193F SD
	4.1	1.01	3	0.8	2.8	0.65
WT ATGL						
Mean SD	P<0.001		P<0.001		P<0.001	
0.3 0.03						
S47A						
Mean SD			P<0.001		P<0.001	
4.1 1.01						
L56R						
Mean SD					P=0.292	
3 0.8						

H

	S47A Mean	S47A SD	L56R Mean	L56R SD	I193F Mean	I193F SD
	8.98	1.23	6.39	0.68	5.87	0.12
WT ATGL						
Mean SD	P<0.05		P<0.05		P<0.05	
3.43 0.26						
S47A						
Mean SD			P<0.05		P<0.05	
8.98 1.23						
L56R						
Mean SD					P=0.262	
6.39 0.68						

Fig. 5. Transient transfection of ATGL mutant proteins in HeLa cells. (A) and (B) Qualitative evaluation of HeLa cells transiently transfected with the following plasmids: pEGFP empty vector (V), p*PNPLA2*-EGFP (WT), p*PNPLA2*(S47A)EFGP, p*PNPLA2*(L56R)EFGP and p*PNPLA2*(I193F)EFGP. LDs stained with ORO are in red. Fluorescence of *PNPLA2*-EGFP recombinant proteins is in green. Images have been captured with immunofluorescent microscope (A) and confocal microscope (B). The cells were analysed for number (C) and dimension (E) – cross section area – of LD per cell. The values represent the means of almost 100 cells for each transfected mutant. (G) Quantification of TG content in HeLa cells transfected with pEGFP empty vector (V), p*PNPLA2*-EGFP (WT), p*PNPLA2*(S47A)EFGP, p*PNPLA2*(L56R)EFGP and p*PNPLA2*(I193F)EFGP. The graph represents TG content from three independent experiments. In (D), (F) and (H) are reported the statistical analysis of data concerning graphs C, E and G. (For interpretation of the references to colour in this figure legend, the reader is referred to the web version of this article.)

results show that these mutations partially impair lipase function. Both L56R and I193F ATGL proteins are able to bind to cytoplasmic lipid droplet and to exert an enzymatic activity, albeit limited if compared with wild type ATGL. The late-onset and slow progression of the myopathy observed in our patients are in agreement with these molecular findings. It must be noted that myocardial dysfunction was not observed in the affected siblings, thus underlining that cardiac involvement could be related to a different degree of biochemical defect [18]. All

patient-carrying missense mutations manifested a milder degree of severity, with the exception of patient described by Coassin et al., in which the p.D166G ATGL mutation directly disrupted catalytic dyad [5,9,10,17–19]. Previous results and those reported in this study show that genotype–phenotype correlation, regarding *PNPLA2* missense mutations and heart disease, should be carefully taken into account to ensure an accurate NLSD-M patient's prognosis, especially when supported by functional studies. Notably, compelling biochemical and molecular approaches, supported by statistical analysis, are highly recommended reporting new cases of enzymes mutations in humans and their metabolic consequences.

In our patients, histochemical inspection of tissues revealed an abnormal accumulation of lipids in muscle fibres, leukocytes and cultured skin fibroblasts. The defect of lipolysis explains the systemic triglyceride storage, distinctive from carnitine deficiency syndrome or other disorders of fatty acid oxidation. The present disorder is accompanied by relatively mild clinical symptoms as compared with carnitine deficiency, while cramps can be also seen in carnitine-palmitoyl-transferase deficiency [23].

In our family, we observed a spectrum of phenotypes, ranging from relatively asymptomatic to full expression of a severe myopathy. This was unexpected considering that the oldest patient and his sister are now in their seventh decade of life (61 and 58 years, respectively). Moreover, they present an asymmetric right-sided muscle involvement of upper and lower limbs. Previous studies have highlighted the predominance of myopathy in the right side [24]. Intra-familiar clinical phenotypic variability emphasises heterogeneity of muscle involvement in spite of similar genetic background. In addition, an unusual liver involvement in the absence of overt clinical muscle weakness, was observed in the female patient. Hepatomegaly and liver steatosis are frequently detected in NLSD-I patients (more than 80%) and are considered as early clinical symptoms together with ichthyosis. Instead, in NLSD-M subjects, liver damage has been noted in only 20% of cases [24], in association with skeletal and cardiac myopathy.

In conclusion, we have found a wide range of intra-familial phenotypic variability in patients carrying the same mutations, both in terms of target-organs and severity of the disease. Currently, molecular knowledge about the biochemical function of ATGL and ABHD5 is incomplete and does not allow us to explain the differences in the clinical manifestations observed in the subject family's members. The enzymatic mechanisms of the lipolytic process and the patho-physiological impact of lipolysis on energy homeostasis in different cell tissues are complex and regulated by extra- or intracellular signalling molecules [2,25]. We may hypothesise that genetic variants and functional polymorphisms of genes other than *PNPLA2* or *ABHD5* can be involved and differently affect clinical manifestation. Moreover, other factors in addition to the genotype may concur to the clinical expression of the disease, such as diet, gender and life style. This rare progressive disorder needs a global collaboration to identify therapeutic strategies and compare clinical phenotypes; for this purpose the international registry for NLSD has been established (www.tgcv.org/r/home.html). In some NLSD-M families with two affected siblings, clinical intra-familial heterogeneity has already been reported. In the subject family, three out of four siblings were affected and showed outstanding differences both in age of onset and clinical symptoms. This study contributes further to the description of the genetic and to widen the clinical spectrum associated with NLSD-M.

Supplementary data to this article can be found online at http://dx.doi.org/10.1016/j.ymgme.2015.05.001.

Acknowledgements

The authors wish to thank the patients for their kind collaboration and Dr. Elisa Colombo for TG quantification analysis. This work was supported by grant GGP14066 from Telethon and BBMRNR part of BBMRI-ERIC. This publication was funded by Università Cattolica del Sacro Cuore among its programmes of promotion and diffusion of scientific research (D.3.1b).

References

[1] M. Schweiger, A. Lass, R. Zimmermann, T.O. Eichmann, R. Zechner, Neutral lipid storage disease: genetic disorders caused by mutations in adipose triglyceride lipase/PNPLA2 or CGI-58/ABHD5, Am. J. Physiol. Endocrinol. Metab. 297 (2009) E289–E296.
[2] R. Zechner, R. Zimmermann, T.O. Eichmann, S.D. Kohlwein, G. Haemmerle, A. Lass, F. Madeo, Fat signals-lipases and lipolysis in lipid metabolism and signalling, Cell Metab. 15 (2012) 279–291.
[3] G.H. Jordans, The familial occurrence of fat containing vacuoles in the leukocytes diagnosed in two brothers suffering from dystrophia musculorum progressiva (ERB.), Acta Med. Scand. 145 (1953) 419–423.
[4] D. Tavian, R. Colombo, Improved cytochemical method for detecting Jordans' bodies in neutral-lipid storage diseases, J. Clin. Pathol. 60 (2007) 956–958.
[5] J. Fischer, C. Lefèvre, E. Morava, J.M. Mussini, P. Laforêt, A. Negre-Salvayre, M. Lathrop, R. Salvayre, The gene encoding adipose triglyceride lipase (PNPLA2) is mutated in neutral lipid storage disease with myopathy, Nat. Genet. 39 (2007) 28–30.
[6] M. Akiyama, K. Sakai, M. Ogawa, J.R. McMillan, D. Sawamura, H. Shimizu, Novel duplication mutation in the patatin domain of adipose triglyceride lipase (PNPLA2) in neutral lipid storage disease with severe myopathy, Muscle Nerve 36 (2007) 856–859.
[7] K. Hirano, A novel clinical entity: triglyceride deposit cardiomyovasculopathy, J. Atheroscler. Thromb. 16 (2009) 702–705.
[8] H.O. Akman, G. Davidzon, K. Tanji, E.J. Macdermott, L. Larsen, M.M. Davidson, R.G. Haller, L.S. Szczepaniak, T.J. Lehman, M. Hirano, S. DiMauro, Neutral lipid storage disease with subclinical myopathy due to a retrotransposal insertion in the PNPLA2 gene, Neuromuscul. Disord. 20 (2010) 397–402.
[9] S. Coassin, M. Schweiger, A. Kloss-Brandstätter, C. Lamina, M. Haun, G. Erhart, B. Paulweber, Y. Rahman, S. Olpin, H. Wolinski, I. Cornaciu, R. Zechner, R. Zimmermann, F. Kronenberg, Investigation and functional characterization of rare genetic variants in the adipose triglyceride lipase in a large healthy working population, PLoS Genet. 6 (2010) e1001239.
[10] D.B. Ash, D. Papadimitriou, A.P. Hays, S. Dimauro, M. Hirano, A novel mutation in PNPLA2 leading to neutral lipid storage disease with myopathy, Arch. Neurol. 69 (2012) 1190–1192.
[11] E.M. Pennisi, S. Missaglia, S. DiMauro, C. Bernardi, H.O. Akman, D. Tavian, A myopathy with unusual features caused by PNPLA2 gene mutations, Muscle Nerve 51 (2014) 609–613.
[12] L. Perrin, L. Féasson, A. Furby, P. Laforêt, F.M. Petit, V. Gautheron, S. Chabrier, PNPLA2 mutation: a paediatric case with early onset but indolent course, Neuromuscul. Disord. 23 (2013) 986–991.
[13] I. Cornaciu, A. Boeszoermenyi, H. Lindermuth, H.M. Nagy, I.K. Cerk, C. Ebner, B. Salzburger, A. Gruber, M. Schweiger, R. Zechner, A. Lass, R. Zimmermann, M. Oberer, The minimal domain of adipose triglyceride lipase (ATGL) ranges until leucine 254 and can be activated and inhibited by CGI-58 and G0S2, respectively, PLoS One 6 (2011) e26349.
[14] K. Kobayashi, T. Inoguchi, Y. Maeda, N. Nakashima, A. Kuwano, E. Eto, N. Ueno, S. Sasaki, F. Sawada, M. Fujii, Y. Matoba, S. Sumiyoshi, H. Kawate, R. Takayanagi, The lack of the C-terminal domain of adipose triglyceride lipase causes neutral lipid storage disease through impaired interactions with lipid droplets, J. Clin. Endocrinol. Metab. 93 (2008) 2877–2884.
[15] P. Laforêt, M. Ørngreen, N. Preisler, G. Andersen, J. Vissing, Blocked muscle fat oxidation during exercise in neutral lipid storage disease, Arch. Neurol. 69 (2012) 530–533.
[16] A. Ohkuma, I. Nonaka, M.C. Malicdan, S. Noguchi, S. Ohji, K. Nomura, H. Sugie, Y.K. Hayashi, I. Nishino, Distal lipid storage myopathy due to PNPLA2 mutation, Neuromuscul. Disord. 18 (2008) 671–674.
[17] P. Reilich, R. Horvath, S. Krause, N. Schramm, D.M. Turnbull, M. Trenell, K.G. Hollingsworth, G.S. Gorman, V.H. Hans, J. Reimann, A. MacMillan, L. Turner, A. Schollen, G. Witte, B. Czermin, E. Holinski-Feder, M.C. Walter, B. Schoser, H. Lochmüller, The phenotypic spectrum of neutral lipid storage myopathy due to mutations in the PNPLA2 gene, J. Neurol. 258 (2011) 1987–1997.
[18] D. Tavian, S. Missaglia, C. Redaelli, E.M. Pennisi, G. Invernici, R. Wessalowski, R. Maiwald, M. Arca, R.A. Coleman, Contribution of novel ATGL missense mutations to the clinical phenotype of NLSD-M: a strikingly low amount of lipase activity may preserve cardiac function, Hum. Mol. Genet. 21 (2012) 5318–5328.
[19] D. Tavian, S. Missaglia, S. DiMauro, C. Bruno, E. Pegoraro, G. Cenacchi, D. Coviello, C. Angelini, A late-onset case of neutral lipid storage disease with myopathy, dropped head syndrome, and peripheral nerve involvement, J. Genet. Syndr. Gene Ther. 4 (2013) 198.
[20] K. Hirano, Y. Ikeda, N. Zaima, Y. Sakata, G. Matsumiya, Triglyceride deposit cardiomyovasculopathy, N. Engl. J. Med. 359 (2008) 2396–2398.
[21] K. Hirano, T. Tanaka, Y. Ikeda, S. Yamaguchi, N. Zaima, K. Kobayashi, A. Suzuki, Y. Sakata, Y. Sakata, K. Kobayashi, T. Toda, N. Fukushima, H. Ishibashi-Ueda, D. Tavian, H. Nagasaka, S.P. Hui, H. Chiba, Y. Sawa, M. Hori, Genetic mutations in adipose triglyceride lipase and myocardial up-regulation of peroxisome proliferated activated receptor-γ in patients with triglyceride deposit cardiomyovasculopathy, Biochem. Biophys. Res. Commun. 443 (2014) 574–579.
[22] V. Dubowitz, C. Sewry, Muscle Biopsy. A Practical Approach, 3rd ed. Saunders Elsevier, 2007.
[23] M. Fanin, A. Anichini, D. Cassandrini, C. Fiorillo, S. Scapolan, C. Minetti, M. Cassanello, M.A. Donati, G. Siciliano, A. D'Amico, F. Lilliu, C. Bruno, C. Angelini, Allelic and

phenotypic heterogeneity in 49 Italian patients with the muscle form of CPT-II deficiency, Clin. Genet. 82 (2012) 232–239.
[24] K. Kaneko, H. Kuroda, R. Izumi, M. Tateyama, M. Kato, K. Sugimura, Y. Sakata, Y. Ikeda, K. Hirano, M. Aoki, A novel mutation in PNPLA2 causes neutral lipid storage disease with myopathy and triglyceride deposit cardiomyovasculopathy: a case report and literature review, Neuromuscul. Disord. 24 (2014) 634–641.
[25] T.C. Walther, R.V. Jr Farese, Lipid droplets and cellular lipid metabolism, Annu. Rev. Biochem. 81 (2012) 687–714.